Int. J. Electrochem. Sci., 12 **(2017)** 1401 – 1420, doi: 10.20964/2017.02.25

International Journal of
ELECTROCHEMICAL
SCIENCE
www.electrochemsci.org

Tobacco Rob Extract as Green Corrosion Inhibitor for N80 Steel in HCl Solution

Yong Guo[1,2], *Meidan Gao*[1], *Hefang Wang*[1,*], *Zhiyong Liu*[1,*]

[1] School of Chemical Engineering and Technology, Hebei University of Technology, Tianjin 300130, China
[2] NOOC Tianjin Chemical Research Design Institute, Tianjin 300131, China
[3] School of Marine Science and Engineering, Hebei University of Technology, Tianjin 300130, China
[*]E-mail: whf0618@163.com, liuzhiyong@hebut.edu.cn

Received: 23 October 2016 / *Accepted:* 6 December 2016 / *Published:* 30 December 2016

The inhibitive action of tobacco rob water extract (TRE) on corrosion of N80 steel in HCl solution was investigated by weight loss, electrochemical measurement, and surface analysis. Results show the main constituents responsible for corrosion inhibition properties of TRE were found to be the nicotine and other components which contain C, O. And a maximum inhibition efficiency of 91.5% is achieved with 750 mg·L^{-1} of TRE in 1M HCl at 60 ℃. Polarization curves reveal that the TRE acts as a mixed-type inhibitor. The values of effective capacitance obtained by electrochemical impedance spectroscopy (EIS) are in the range of double layer capacitance. The adsorption behavior of TRE follows Langmuir adsorption isotherm and the activation parameters governing adsorption process were calculated and discussed.

Keywords: tobacco rob extract, corrosion inhibitor, polarization, EIS

1. INTRODUCTION

Acid solutions are often used in drilling operations in oil and gas exploration, as well as for cleaning, descaling and pickling of steel structures. These processes are normally accompanied by considerable dissolution of the metal. Among the acids, hydrochloric acid (HCl) is one of the most widely used agents in several industries for the removal of undesirable oxide films and corrosion products of the steel surface. One of the most common, effective and economic methods to prevent metal dissolution in acidic environment is the use of corrosion inhibitors.

Heterocyclic organic compounds containing O, S, and N atoms are used as corrosion inhibitors for steel in acid environments. Many synthetic compounds are used as corrosion inhibitors in various media [1-5]. However, most of the traditional synthetic compounds inhibitors are toxic, high operating

cost and unenvironmental friendly during their synthesis and use [6]. So scientists have focused their research on green corrosion inhibitors in recent years. Natural plant is inexpensive, eco-friendly and renewable sources of materials. So it is interesting to study nature plant as an effective and economic corrosion inhibitor if it has high inhibition efficiency. Therefore, finding naturally occurring substances as corrosion inhibitors is of great practical significance [7-11]. Hence, investigations are focused on the development of naturally occurring substances as eco-friendly corrosion inhibitors [12-18]. A few of alkaloids extract from plants, such as Kopsia singapurensis [19], Annona squamosa [20], Aspidosperma album [21], Oxandra asbeckii [8], Palicourea guianensis [10], Geissospermum laeve [22] have been reported as good inhibitors in HCl solution.

Tobacco plants were widely cultivated in the world as an important cigarette material. The tobacco production was 500-550 million tons in China each year. Tobacco rob (TR) accounts for more than 60% of the total tobacco plants production, which is useless for cigarette production. TR was usually burned as agricultural waste, which led to serious environmental problems and enormous waste of resources. So the reutilization of the waste and the exploitation for potential bio-energy would be promising [23, 24]. More than 4,000 individual constituents have been identified in tobacco including organic acids, phenolic compounds, carbohydrate compounds, nicotine et al. Nicotine is the major alkaloid constituent of the plant [25-29]. A few previous works reported inhibition property of tobacco and cigarette butts as corrosion inhibitor in saline solutions or HCl solution [25-28]. However, previous reports had no information on the active ingredients that are responsible for the corrosion inhibition.

Our previous work showed that TRE had good scale and corrosion inhibition properties for carbon steel in circulating cooling water [30]. The objective of the present work is to study the inhibitive action of TRE as a cheap, green and naturally occurring substance on corrosion behavior of N80 steel in HCl. The inhibitive action of TRE was investigated by weight loss and electrochemical measurement. The main constituents responsible for corrosion inhibition properties of TRE were found. The FT-IR, SEM and XPS were used to further confirm TRE adsorption on the N80 surface.

2. EXPERIMENTAL

2.1. Preparation of TRE

The dried TR powder (8.0 g) was soaked in flask of three necked with distilled water (100 mL) and refluxed for 2 h. After cooling to room temperature, the extract was filtered and then diluted to 100 mL. The residue was dried at 105 ℃ (removal of water) for 12 h. From the weight of the dried residue, the concentration of extract was 34 $mg \cdot mL^{-1}$.

2.2. Preparation of specimens

N80 steel coupons with composition (wt %) of 0.24 C, 1.58 Mn, 0.012 S, 0.32 Si, 0.022 P, 0.05 Ni and remaining Fe were polished successively using different grades of emery papers (grade Nos. 240, 600), degreased with acetone, washed with distilled water and then ethanol before the experiment.

3. EXPERIMENTAL METHODS

3.1. Weight loss method

Weight loss of N80 steel coupons (40 mm× 13 mm× 2 mm) immersed in 500 mL aqueous of HCl in the absence and presence of different concentrations of TRE was determined at 25 ℃, 45 ℃ and 60 ℃. All experiments were carried out in aerated and static conditions. The corrosion rate (Vi) of N80 steel was calculated from the following equation:

$$V_i = \frac{10^6 \times \Delta m_i}{A_i \times \Delta t} \quad (1)$$

Where V_i is the corrosion rate of N80 steel ($g \cdot m^{-2} \cdot h^{-1}$), Δm_i is the average weight loss of N80 steel (g), A_i is the total area of the N80 steel specimen (m^2), and Δt is the immersion time (h).

The inhibition efficiency (IE) was calculated using the following equation:

$$IE(\%) = \frac{V_0 - V}{V_0} \times 100 \quad (2)$$

where V_0 and V are the corrosion rates of N80 steel specimens in the absence and presence of TRE, respectively.

3.2. Electrochemical measurements

CHI660E electrochemical analyzer was used to electrochemical measurements according to ASTM standards. Electrochemical measurements were performed at 60 ℃ with three electrodes system. A platinum sheet and a saturated calomel electrode (SCE) were used as auxiliary and reference electrodes, respectively. All the potentials reported were with reference to SCE. The working electrode was a square cut from N80 with surface area 1 cm^2. The working electrode and the reference electrode are connected via a salt bridge. In order to minimize the ohmic voltage error, the salt bridge was as close as possible to the electrode surface. Before measurements, the working electrode was polished mechanically, washed with acetone, rinsed several times with distilled water and dried.

The open circuit potential (Eocp) was obtained in a stable state, which was achieved after 60 min before the electrochemical measurements. The potentiodynamic polarization measurements conducted separate scans from open circuit potential (Eocp) at scan rate of 0.57 $mV \cdot s^{-1}$. EIS measurements were performed at frequencies of 10 kHz to 100 mHz with an alternative (AC) amplitude of 10 mV signal from the Eocp. The charge transfer resistance (Rt) and the double layer capacitance values (C_{dl}) were obtained from EIS. IE obtained from EIS was calculated with the following equation:

$$IE\% = \frac{R_{ct} - R_{ct^0}}{R_{ct}} \times 100 \quad (3)$$

$$\theta = \frac{R_{ct} - R_{ct^0}}{R_{ct}} \quad (4)$$

where Rct and Rct^0 is the charge transfer resistance in the presence and absence of TRE, respectively, and θ is surface coverage value.

3.3. Infrared spectroscopy

Fourier transform infrared spectroscopy (FT-IR) spectra were recorded using FT-IR spectrometer (BRUKER TENSOR 27). The spectra for TRE and the protective film formed on the N80 steel surface after 4 h immersion in 1 M HCl solutions containing 1500 $mg \cdot L^{-1}$ of TRE using the KBr pellet technique.

3.4. Surface analysis

The test coupons were immersed in 500 mL of 1 M HCl with 1500 $mg \cdot L^{-1}$ TRE for 4 h at 60℃ and washed with distilled water. After washing, specimens were examined for their structural and topographical features using scanning electron microscope (SEM NOVA NA NOSEM 450) and X-ray photoelectron spectroscopy (XPS Uivac-Phi PHI5000 VersaProbe).

4. RESULTS AND DISCUSSION

4.1. Constituent responsible for inhibition

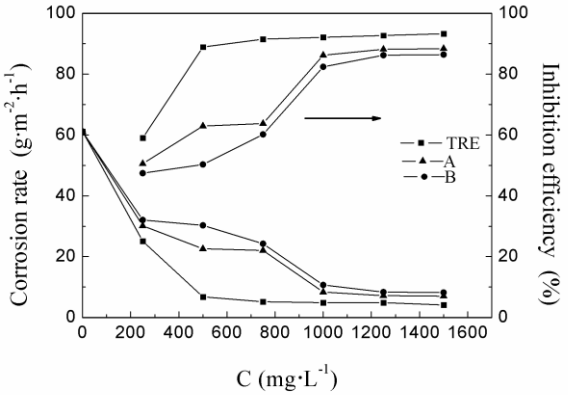

Figure 1. The corrosion rate and the IE of N80 steel in the presence of different concentrations of TRE, A: Nicotine (Separated from TRE by extracting using chloroform as extractor) and B: (TRE after removal of nicotine).

Nicotine (A) was separated individually from TRE by extracting TRE, using chloroform as extractor according to the previous work [8, 10, 20, 21]. Fig. 1 shows the corrosion rate and IE of N80 steel in the absence and presence of different concentrations of TRE, A and B (B: after removal of nicotine from TRE) immersed in 1 M HCl at 60 ℃. Clearly, the maximum IE of TRE, A and B is 93.3%, 88.4%, and 86.5%, respectively. The obtained results indicate that both the constituents of A

and B have corrosion inhibition. In addition, IE in the same concentrations of A is higher than B, which indicates A is the main constituents responsible for inhibition. However, IE with the same concentrations of TRE is much higher than those of A and B. So the inhibition performance of TRE was investigated in our study.

4.2. Analysis of TRE

Gas chromatography-mass spectroscopy (GC-MS TRACE DSQ) analysis of TRE showed the presence of organic acids (3.15 wt %) [31]. High performance liquid chromatography (HPLC SHIMADZU LC-10A) analysis of TRE showed the presence of phenolic compounds (2.78 wt %) [32] and total carbohydrate compounds (65.4 wt %) [33]. Ultraviolet -visible absorption spectrometry (UV INESA L5) analysis of TRE showed presence of nicotine (4.20 wt %) [29].

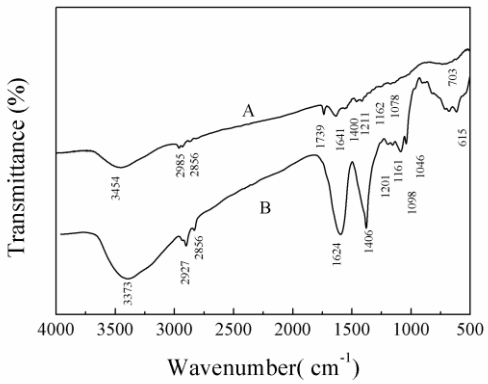

Figure 2. FT-IR spectra of samples: (A) TRE adsorbed on N80 steel, (B) TRE.

Fig. 2 shows the FT-IR spectra of the TRE and the TRE adsorbed on N80 steel. The typical peaks of FT-IR are presented in Table 1. The absorption band at 3373 cm^{-1} is attributed to N-H or O-H bond stretching vibration [34]. The peaks at 2927 cm^{-1} and 2856 cm^{-1} are attributed to stretching mode of aliphatic and aromatic C-H groups respectively [12, 34]. The peaks at 1624 cm^{-1} corresponds to C=O attached to amino group [35]. The peaks at 1201 cm^{-1} is attributed to the framework vibration of aromatic ring [34], which implies the presence of Aryl OH. The absorbance at the 1161 cm^{-1} is assigned to stretching mode of C-O [36]. The band at 1098 cm^{-1} and 1046 cm^{-1} is due to the stretching mode of C-N (tertiary amine) [12]. Therefore, it can be inferred that TRE contains oxygen and nitrogen atoms in functional groups (O-H, N-H, C-N, C=O, C-O), which may have inhibition property. Almost all peaks for TRE are also observed in the FT-IR spectrum of TRE adsorbed on N80 steel. The peak at 1739 cm^{-1} indicates the presence of Iron-plant extract complex or salt [36, 37]. The band at 703 cm^{-1} probably originates from γ-Fe_2O_3 [36]. The results of FT-IR indicate that the components of TRE were adsorbed on the metal surface. This indicates that nicotine (Fig. 3) and other contain C, O constituents of TRE are responsible for corrosion inhibition property.

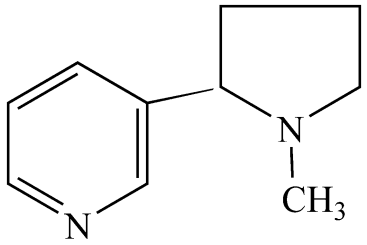

Figure 3. Molecular structure of Nicotine

Table 1. Peaks from FT-IR spectra of samples: (A) TRE adsorbed on N80 steel, (B) TRE

Wavenumber(cm^{-1})		Possible groups	Reference
N80 in TRE	TRE		
3454	3373	O—H/N—H	[27, 38]
2985	2927	Aliphatic C—H	[12, 36]
2856	2856	Aromatic C—H	[12, 36]
1739	-	C=O complexed with metal cation	[36, 37]
1641	1624	$\overset{O}{\overset{\|}{R}}C—NH_2$ C=O attach to amino group (Alkaloids)	[35]
1400	1406	$—\overset{O}{\overset{\|}{C}}—OM$	[35]
1211	1201	Aryl OH（Hydrogen bonding）	[12]
1162	1161	C—O	[36]
1078	1098、1046	C—N Tertiary amine (Nicotine)	[12, 11]
703	-	γ—Fe_2O_3	[36]

4.3. Effect of acid concentration

Fig. 4 shows the corrosion rate and the IE of N80 steel immersed in 1 M-5 M HCl in the absence and presence of different concentrations of TRE at 60 ℃. The corrosion rate of N80 steel dramatically decreases with increase of TRE concentration, while the IE increases. The corrosion rate of 5.18 $g \cdot m^{-2} \cdot h^{-1}$ and IE of 91.5% are obtained in 1 M HCl solution with 750 $mg \cdot L^{-1}$ TRE. No appreciable increase in IE was noticed above this concentration. While the corrosion rate increases dramatically and IE of N80 steel decreases with increase in acid concentration from 1 M to 5 M.

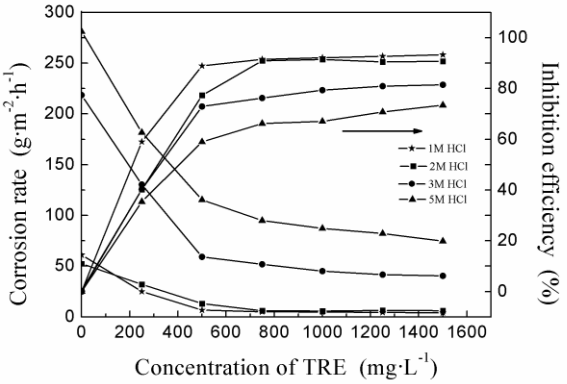

Figure 4. Effect of different concentrations of TRE on corrosion rate and IE at 60 ℃ in 1 M-5 M HCl.

4.4. Effect of immersion time

It is necessary to investigate the effect of immersion time on IE to study the stability of inhibitive behavior. Fig. 5 shows the effect of immersion time (0.5-24 h) on corrosion inhibition with 750 mg·L^{-1} of TRE in 1 M HCl at 60 ℃ using the weight loss method. The results showed IE firstly increased with immersion time from 0.5 to 4 h, and reached maximum value at 4 h (91.5%), then no increase with immersion time prolonging to 24 h. The reasons could be attributed to the adsorptive film of TRE that formed in the immersion [22, 39]. The adsorptive film becomes more compact and uniform from 0.5 h to 4 h, and with prolonging of immersion time (4-24 h), the adsorptive film achieves saturated adsorption within 4-24 h [40]. Therefore, the IE initially increases with time and then remains constant during the investigated time.

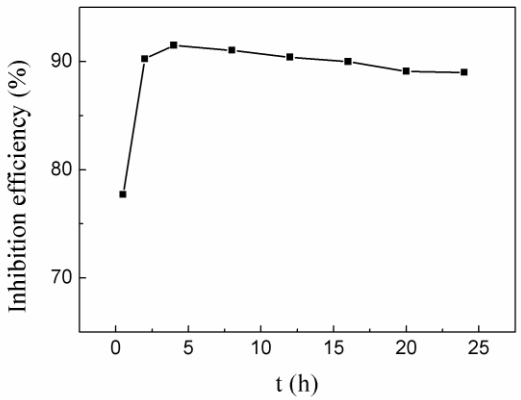

Figure 5. Effect of immersion time on IE with TRE in 1 M HCl at 60 ℃ using the weight loss method.

4.5. Effect of temperature

The effect of temperature on the inhibitive performance of TRE was studied by weight loss method. Fig. 6 shows the corrosion rate and the IE in 1 M HCl at 25 ℃, 45 ℃ and 60 ℃. Results showed a remarkable increase in N80 steel corrosion rate with increase of temperature. The corrosion rate decreased with the concentration of TRE increased and the IE increased with increase in

temperature in the presence of TRE. The IE increases from 86.5% to 91.5% with the increase of temperature form 25 ℃ to 60 ℃ with 750 mg·L^{-1} of TRE. The increase in IE with increase of temperature confirms that chemisorption of the TRE components onto the N80 steel surface [41-44]. Chemisorption of the TRE components provides more effective protection because of reduction the reactivity of the metal at the sites where they are attached [45].

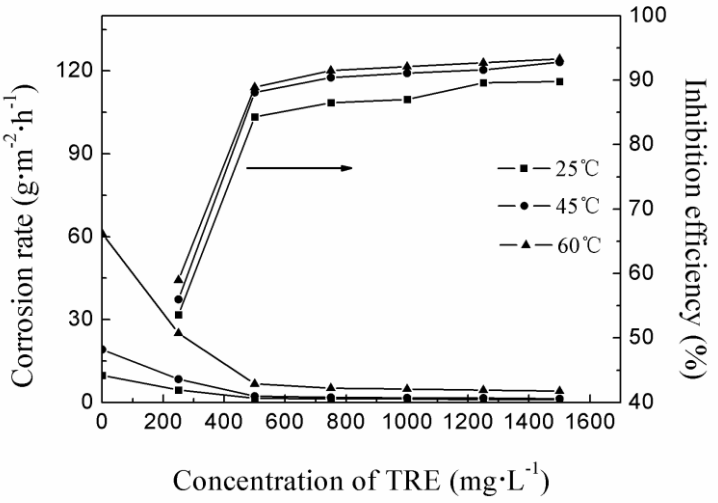

Figure 6. Effect of TRE concentration and temperature on IE and corrosion rate in 1 M HCl at 25 ℃, 45 ℃ and 60 ℃.

4.6. Activation energy calculations

The apparent activation energy (Ea) for the corrosion process in absence and presence of TRE was evaluated from Arrhenius equation [7, 46]

$$lnv = -\frac{Ea}{RT} + lnA \quad (4)$$

where V is the corrosion rate, A is the Arrhenius pre-exponential constant, Ea is the activation corrosion energy for the corrosion process, R is the gas constant and T is the absolute temperature.

Fig. 7 shows the plotting natural logarithm of the corrosion rate versus 1000/T. The activation energy can be calculated from the slope. The calculated values of Ea of TRE are listed in the Table 2. It is clear that Ea values in the presence of the different concentrations of the extract are lower than that without TRE. The decrease in apparent activation energy in the presence of the extract indicates chemical adsorption, which is in agreement with the above results of temperature on IE and corrosion rate (Table 2).Similar result has also been reported by Ating et al during the study of inhibition performance of Ananas sativum for aluminum in hydrochloric[47]. The whole process is controlled by surface reaction since the energy of activation of the corrosion process are greater than 20 kJ·mol^{-1}, which is in accordance with the obtained results of Krishnegowda [48].

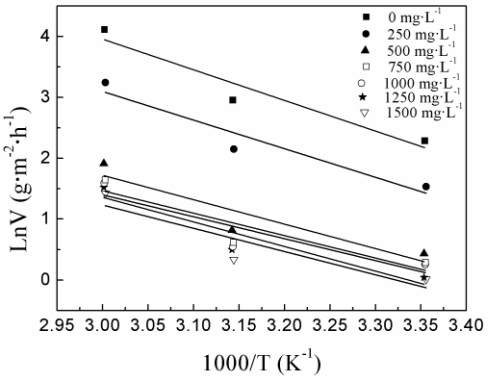

Figure 7. Variations of LnV with 1000/T in 1 M HCl with and without TRE.

Table 2. Calculated values of activation parameters for corrosion of N80 steel in 1 M HCl

C/(mg·L^{-1})	Slope	LnA/(g·m^{-2}·h^{-1})	Ea/(kJ·mol^{-1})
0	-5.03	19.1	41.8
250	-4.69	17.1	39.0
500	-4.01	13.8	33.3
750	-3.69	12.5	30.7
1000	-3.61	12.2	30.0
1250	-4.04	13.4	33.6
1500	-3.81	12.7	31.7

The increase of temperature accelerates the chemisorption of the TRE of the metal surface. The results of the FT-IR reveal the TRE contain nicotine and other contains C, O constituents. The constituent contain N and O atoms in their molecules, which are regarded as centers of adsorption [47, 49]. The adsorption of TRE on the N80 steel surface can also be explained on the basis of the donor-acceptor interaction between π- electrons of donor atoms N of the inhibitors and the vacant d-orbital's of iron surface atoms. The adsorption compounds of TRE on the N80 surface by the chemisorption mechanism, involving the coordinate bonds formed between the lone electrons pairs of the unprotonated N atoms and the empty d-orbital of Fe atoms, enhanced the combination between TRE and electrode surface. The adsorption of TRE on the N80 surface makes a barrier for mass and charge transfers. Consequently, the metal is protected from the aggressive of the acid [47].

4.7. Open circuit potential

The variation of open circuit potential with time for N80 in 1 M HCl with different concentrations of TRE is shown in Fig. 8. A stable OCP values were obtained after 3600 s immersion both in the absence and presence of TRE. It is also observed that the potentials with TRE shift to positive values in comparison with that of without TRE. The positive shift of corrosion potential was

found to be dependent on concentration, which suggests a possible influence of TRE on both anodic and cathodic polarization.

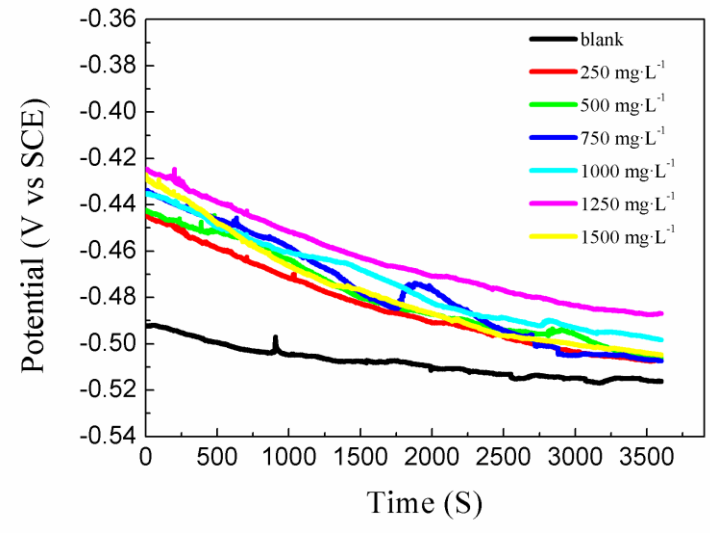

Figure 8. OCP curves for N80 steel in 1 M HCl in different concentration of TRE.

4.8. Potentiodynamic polarization measurements

In order to know the kinetics of anodic and cathodic reactions, potentiodynamic polarization experiments were carried out in 1 M HCl solution in the presence of different concentration of TRE at 60 ℃. The experiments were performed from OCP in upwards scans and separately in downward scans according to ASTM. The obtained polarization curves are shown in Fig. 9. The electrochemical parameters and IE are listed in Table 3. Both reaction rates are balanced at the intersection of anodic polarization curve and cathodic polarization curve. This intersection is the corrosion current density (Icorr).

Fig. 9 shows that there is no significant change in the Eocp values in the presence and absence of the TRE. An inhibitor is classified as cathodic or anodic type if the displacement in corrosion potential is more than 85 mV with respect to corrosion potential of the blank [28, 50-52]. But in this study, the largest displacement exhibited of the TRE was 24 mV, from which it can be concluded that TRE acts as a mixed type inhibitor. This is also in agreement with the conclusion of open circuit potential. Fig. 9 also shows both the anodic and the cathodic reactions are suppressed, suggesting that the Fe dissolution reaction is reduced and also the hydrogen reduction is retarded, which is in agreement with Bockris, Drazic and Despic (BDD mechanism) [53]. Additionally, Icorr decreased when the TRE concentration increased, suggesting that TRE is a good corrosion inhibitor for N80 steel in 1 M HCl solution.

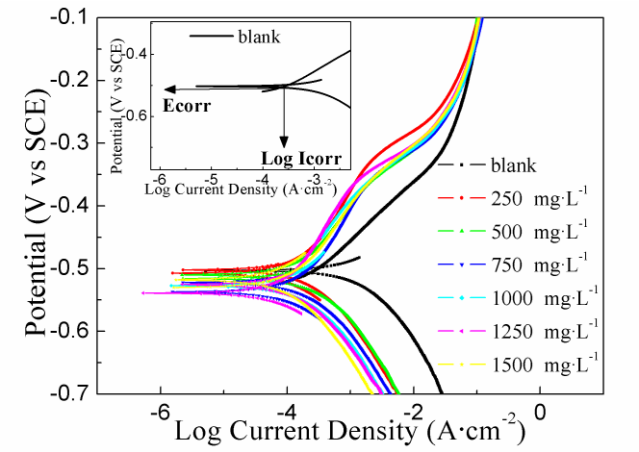

Figure 9. Polarization curves for N80 steel immersed in 1 M HCl with and without TRE at 60 ℃.

Table 3. Polarization parameters and IE for the corrosion of N80 at different concentrations of TRE

C(mg·L^{-1})	Eocp(V vs SCE)	Icorr(10^{4}A·cm^{-2})	IE%
Blank	-0.507	2.28	-
250	-0.516	1.11	51.3
500	-0.526	0.912	60.0
750	-0.528	0.504	77.9
1000	-0.522	0.331	85.5
1250	-0.531	0.319	86.0
1500	-0.524	0.280	87.7

4.9. EIS measurements

The kinetics of the electrochemical processes and capacitive behaviors at 1 M HCl/steel interface in the presence and absence of TRE were evaluated by EIS. Fig. 10 show the Nyquist (a), Bodes' modulus (b) and phase angle plots (c) for TRE. From Nyquist plots, it shows that the electrochemical response of N80 steel appeared in form of depressed capacitive loops, suggesting that a capacitive layer was formed at HCl/steel interface. The diameters of semi-circles increased with concentration of the extracts indicating that charge transfer process at the interface retarded in presence of TRE [54]. The Bode phase angle plots of TRE show only one relaxation process, which are in agreement with one semi-circle capacitive loop in the Nyquist plots over the range of frequencies. This behavior is attributed to a time constant in an electrochemical system according to the report of Odewunmi[55].

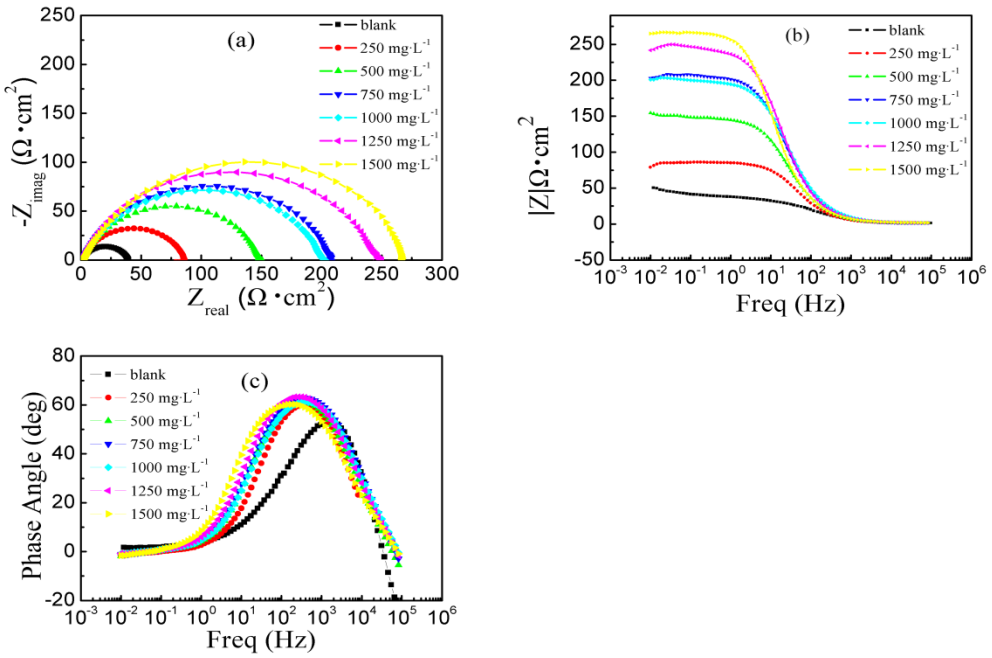

Figure 10. Impedance plots for N80 steel in 1 M HCl in different concentrations of TRE; (a) Nyquist, (b) Bode modulus and (c) Bode phase angle at 60 ℃.

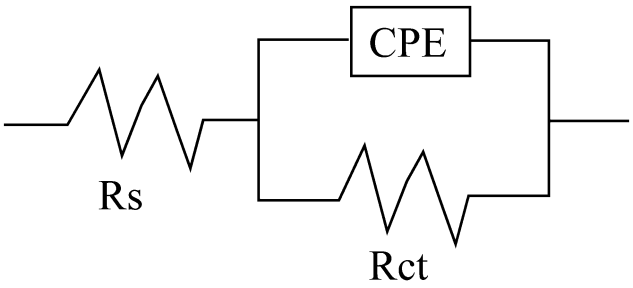

Figure 11. Equivalent circuit for the EIS data fittings.

To investigate technical details of impedance spectra, Fig. 11 shows an equivalent electrochemical circuit. A constant phase element (CPE) should be introduced to replace a true capacitor in the equivalent circuit to account for the effect in order to estimate the impedance parameters [56] and its impedance is expressed as follows :

$$Z_{CPE} = \left[Y_0 (j\omega)^n\right]^{-1} \quad (5)$$

where Y_0 is the magnitude of the CPE, ω is angular frequency and n is a physical parameter which signifies interface surface properties of working electrode. For n = 0, Z_{CPE} represents a resistance; for n = 1, a capacitance; for n = -1, an inductance. The C_{dl} is calculated from Y_0 and n using the following equation: [48]

$$C_{dl} = \left(Y_0 R_{ct}^{1-n}\right)^{1/n} \quad (6)$$

The impedance parameters such as solution resistance Rs, charge transfer resistance Rct, double layer capacitance C_{dl}, magnitude of constant phase element (CPE) Y_0 and n are obtained from the simulation of experimental impedance data by ZSimpWin software and given in Table 4.

Table 4. EIS parameters of N80 steel in 1 M HCl in the absence and presence of TRE

C ($mg \cdot L^{-1}$)	Rs ($\Omega \cdot cm^2$)	Rct ($\Omega \cdot cm^2$)	n	Y_0 ($10^6 \Omega^{-1} \cdot s^n \cdot cm^{-2}$)	C_{dl} ($\mu F \cdot cm^{-2}$)	IE%	θ
0	1.14	38.6	0.80	213	64.0	-	-
250	1.64	74.6	0.85	133	58.9	48.3	0.483
500	1.56	148	0.81	137	54.9	73.9	0.739
750	1.51	206	0.81	112	46.3	81.3	0.813
1000	1.76	207	0.79	114	42.1	81.4	0.814
1250	1.69	251	0.80	103	41.3	84.6	0.846
1500	1.96	271	0.78	104	38.0	85.8	0.858

Table 4 shows that Rct values increased with increase of TRE concentration while C_{dl} values decreased, which was attributed to the displacement of water molecules by the adsorbed species of TRE onto the N80 steel surface, resulting increase in double layer thickness lead to decrease in the dielectric constant [57]. Also the IE increased with increase in TRE concentration. This indicates the adsorption of nicotine and other components containing C, O onto the N80 steel surface could prevent the attack of corrosive solution by creating a barrier for mass and charge transfer. The n values are close to unity, which suggests that the CPE is related to the capacitance and the dissolution mechanism of N80 in HCl is controlled by charge transfer process. The IE obtained from EIS is in good correspondence with the data obtained by potentiodynamic polarization. However, the IE obtained from the weight loss method is higher than those obtained from EIS measurements and potentiodynamic polarization tests. The discrepancy in IE obtained is mainly due to that electrochemical technique gives instantaneous corrosion rate, while weight loss method provides average corrosion rate [58]. These differences are probably due to the different exposure time in the corrosive solution. The high IE indicates a strong adsorption favored by the long duration of the experiments. Therefore, the weight loss experiments confirmed the electrochemical results regarding the adsorption of TRE on N80 steel surface. This phenomenon was also observed by the report of Souza [59].

4.10. Adsorption isotherms

Adsorption isotherms are very important in the study of the mechanism of organo-electrochemical reaction. The EIS experimental data was utilized to obtain useful information on the nature of adsorption of TRE on N80 surface in 1 M HCl at 60 ℃ via adsorption isotherms. Attempts were made to fit experimental data with several adsorption isotherms like Langmuir, Temkin, Frumkin and Freundlich isotherms. However the best fit was obtained with Langmuir isotherm, which is in good agreement with the equation [60]:

$$\frac{C}{\theta} = \frac{1}{K} + C \quad (7)$$

where C is the TRE concentration. θ is the degree of surface coverage, which have been calculated by EIS and K is the equilibrium constant of adsorption process.

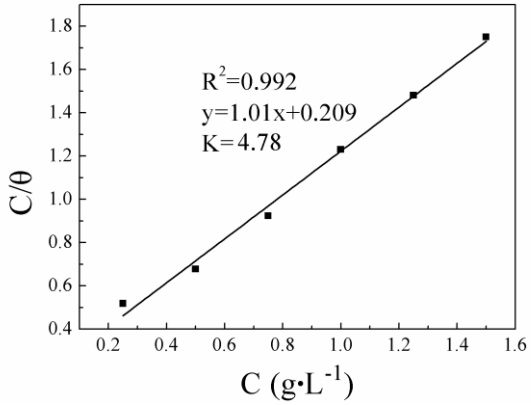

Figure 12. Langmuir adsorption isotherms for TRE in 1 M HCl on N80 steel.

Table 5. Comparison of the IE of TRE with other natural products extracts for steel in acidic media at 60 ℃

Natural Products	Metal exposed	Acidic medium	Concentration of extract	IE (%)	Reference
tobacco rob	N80	1M HCl	0.75 g·L^{-1}	91.5[a]	present
Tagetes erecta	Mild steel	0.5 M H_2SO_4	1.0 g·L^{-1}	40.0[c]	[11]
Acalypha torta	Mild steel	1 M HCl	1.0 g·L^{-1}	72.0[a]	[47]
Bark of N. latifolia	Mild steel	5.0 M H_2SO_4	4.0 g·L^{-1}	70.1[b]	[50]
leaves of N.				71.6[b]	
root of N. latifolia				72.0[b]	
Mango peel	C-steel	1 M HCl	0.4 g·L^{-1}	62.0[a]	[16]
Orange peel				80.0[a]	
Passion fruit peel				72.0[a]	
Cashew peel				50.0[a]	
Henna	Mild steel	1 M HCl	1.2 g·L^{-1}	37.9[a]	[7]
Pachylobus edulis	aluminium	0.1 M HCl	0.5 g·L^{-1}	34.0[a]	[39]
Raphia hookeri				46.1[a]	

a Values from the weight loss method. b Values from the gasometric measurements. c Values from electrochemical impedance spectroscopic measurement

The plots of C/θ versus C were straight lines with almost unit slopes and calculation results and parameters are given in Fig. 12. It is found that the regression coefficient is close to one, which indicates that adsorption of nicotine and other components containing C, O of TRE on the N80 steel surface obeys Langmuir adsorption isotherm. Langmuir isotherm assumes that the solid surface contains a fixed number of adsorption sites and each site holds one adsorbed species [61]. The adsorption occurred on specific homogenous sites on the metal surface and was successfully used in monolayer adsorption process. This indicates that the adsorbed species of TRE occupies typical adsorption site at the metal/solution interface.

Table 5 shows comparison of the IE of TRE with those of other natural products extracts for steel in acidic media at 60 ℃. The results show that the IE of TRE reached 91.5% at a relatively low concentration (0.75 $g \cdot L^{-1}$) in 1M H^+ solution. However, the IE of Tagetes erecta and Acalypha torta leaves (1.0 $g \cdot L^{-1}$) were only 40.0% and 72.0%, respectively. The IE of Bark of N. latifolia, leaves of N. latifolia, root of N. latifolia (4.0 $g \cdot L^{-1}$), Henna (1.2 $g \cdot L^{-1}$) and several fruit peel (0.4 $g \cdot L^{-1}$) were no more than 80.0%. Table 5 also shows that the IE of Pachylobus edulis and Raphia hookeri (0.5 $g \cdot L^{-1}$) were 34.0% and 46.1%, respectively in 0.1M HCl solution. A comparison of these data with the results of present investigation reveals that TRE is an effective corrosion inhibitor [14, 39].

4.11. Surface analysis of N80 steel surface exposed to TRE

SEM images of N80 steel (Fig. 13a), N80 steel immersed in 1 M HCl solution in the absence (Fig. 13b) and presence of 1500 $mg \cdot L^{-1}$ TRE (Fig. 13c) are shown in Fig. 13. Fig. 13a exhibits finely polished characteristic surface of N80 steel and shows some scratches due to polishing. Fig. 13b reveals that the specimen surface is strongly damaged in the absence of the TRE in 1 M HCl. With the presence of TRE (Fig. 13c), the specimen has smooth surface compared with that of without TRR, which indicates that the constituents of TRE (nicotine and other components which contain C, O) hinders the dissolution of iron and there by reduces the corrosion rate of N80 steel in HCl solution.

The X-ray photoelectron spectroscopy (XPS) measurement is performed to obtain information on the surface coverage of the TRE after the weight loss. Fig. 14 shows XPS spectra of Fe2p, O1s, N1s and C1s for the N80 steel specimen after immersion for 4h in 1 M HCl solution containing 1500 $mg \cdot L^{-1}$ TRE. The binding energies of elements along with their intensities are given in Table 6.

The Fe2p spectrum exhibits two doublets, 711.0 eV (Fe2p3/2) and 724.5 eV (Fe2p1/2) with an associated ghost structure on the high energy side, which indicates the oxidation of N80 steel surface. The deconvolution of the high resolution Fe 2p3/2 XPS spectrum (711.0 eV) consists three peaks at 707.1, 710.7

and 715.5 eV. The peak at 707.1 eV is attributed to metallic iron. The BE at 710.7 eV is assigned to Fe^{3+}, which is associated to ferric oxide/hydroxide species such as Fe_2O_3/Fe_3O_4 and FeOOH [62], reducing ions diffusion and improving the corrosion resistance of N80 steel in HCl solutions. The last peak at 715.5 eV was partly ascribed to the satellite of Fe(III) [63] and partly related to the presence of a small concentration of $FeCl_3$ on N80 steel surface due to the presence of HCl [64].

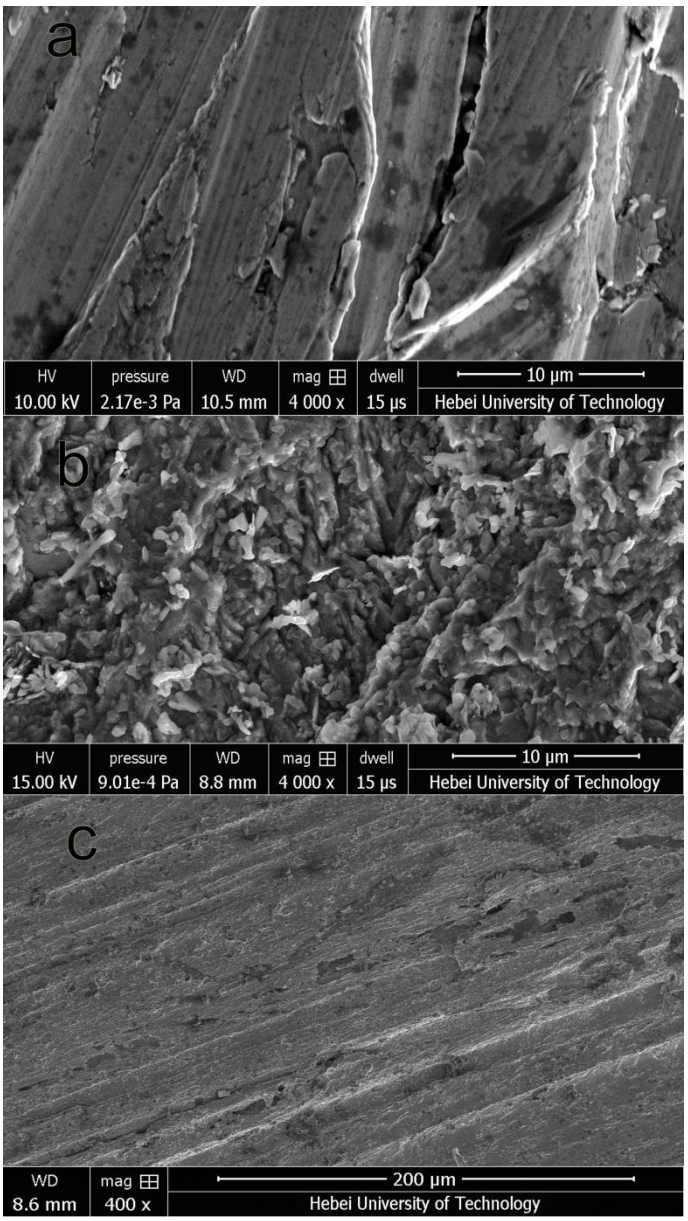

Figure 13. SEM graphs of N80 steel: (a) polished surface (b) N80 steel immersed in 1 M HCl and (c) N80 steel immersed in 1 M HCl with 1500 mg·L^{-1} of TRE.

The O1s spectrum is deconvoluted labeled as 1 and 2, which are correspond to the binding energy of the O^{2-} and OH^-, indicating the presence of the iron oxide/hydroxide layer as detected in the Fe 2p3/2spectrum. The peak 1(529.5 eV) is ascribed to O^{2-} and relates to oxygen atoms bonded to Fe^{3+} in the Fe_2O_3 and/or Fe_3O_4 oxides [65]. Peak 2 (531.2 eV) is attributed to OH^-, which associates to the presence of hydrous iron oxides, such as FeOOH [65]. Indeed, the corresponding N 1s spectrum can be deconvoluted into two peaks, the first peak at 399.6 eV is mainly attributed to the bonds of C-N and the unprotonated N atoms (=N- structure) [62]. The second peak may be attributed to positively charged nitrogen, probably due to the protonated nitrogen atoms in the nicotine molecule [66]. In addition, compared with unprotonated =N-, the second peak shifts to high binding energy with the formation of the N-Fe bond complex [5]. The peak of the organic nitrogen group appeared at slightly higher position because of the adsorption of TRE to the N80 steel surfaces. The shift in N 1s spectrum

clearly indicates that complex formed directly on the basis of donor acceptor interactions between N atoms of the neutral species and the vacant d orbital of iron. Their presence demonstrates that TRE molecules are adsorbed on N80 surface. This is in agreement with the C 1s region, whose peaks are due to C-H, C-C, C-N and/ or C=N and C-N^+ or C=N^+ bonds. The C 1s spectrum was deconvoluted to three components, labeled as 1, 2 and 3. The peak at 285.0 eV is attributed to C-H, C-C and C-H bonds from TRE molecules [5]. The peak at 286.7 eV is ascribed to C-N and/ or C=N [66]. The third peak at 289.0 eV can be attributed to C-N^+ or C=N^+. This result also supports the presence of adsorbed TRE on the N80 steel surface.

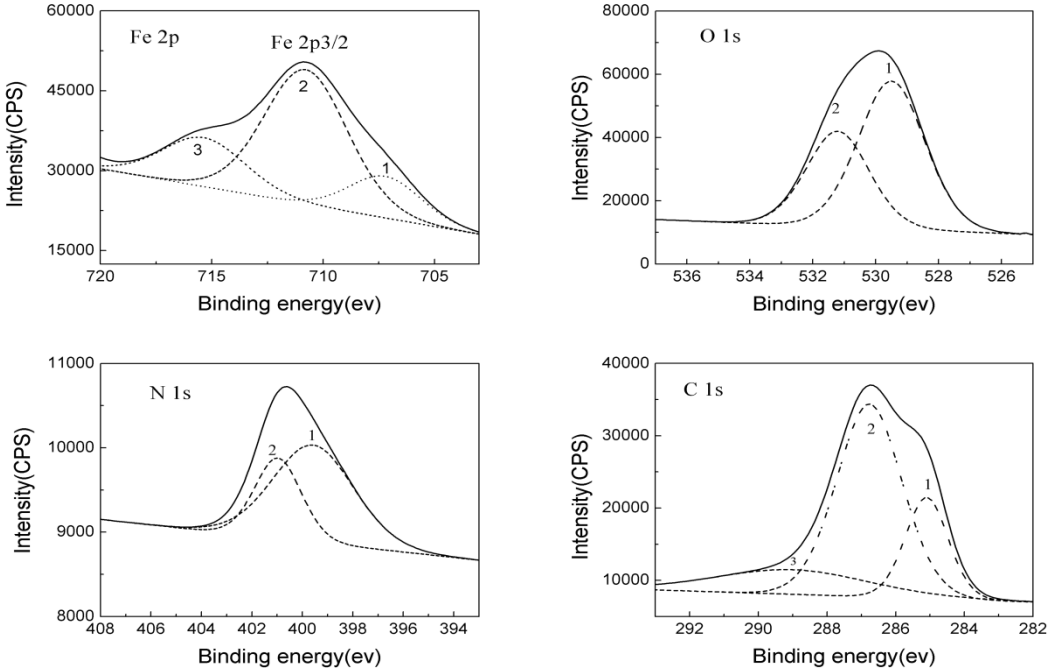

Figure 14. X-ray photoelectron spectra of N80 steel after immersion for 4h in 1 M HCl solution containing 1500 mg·L^{-1} TRE.

Table 6. Binding energies and relative intensities of N 1s, C 1s, O 1s and Fe 2p3/2 from XPS

Electron	Species	Binding energy(eV)	Relative intensity(CPS)
N 1s	1	399.6	67.8
	2	400.9	32.2
C 1s	1	285.0	20.9
	2	286.7	60.8
	3	289.0	18.3
O 1s	1	529.5	62.2
	2	531.2	37.8
Fe 2p3/2	1	707.1	14.0
	2	710.7	66.1
	3	715.5	19.9

The XPS results provide direct evidence of the adsorption of TRE molecules onto N80 surface and corroborate the thermodynamic study. The above results show that the inhibitive film formed on the N80 steel surface contains iron extract complex having C, O and N atoms. This confirms again that the formed corrosion inhibitive layer contains nicotine, also suggesting chemical interactions between the nicotine and other components of TRE on N80 steel surface. Thus, nicotine and other components containing C, O act as inhibitor for corrosion inhibition on N80 steel.

5. CONCLUSIONS

From the experimental results and discussion in this work, the following conclusions can be deduced. The main constituents responsible for corrosion inhibition of TRE were found to be nicotine and other components containing C, O. The IE of N80 steel increases with increase of TRE concentration and decrease of acid concentration. 91.5% IE in 1 M HCl was obtained with 750 $mg \cdot L^{-1}$ TRE at 60 ℃. TRE is effective in reducing corrosion rate of N80 steel in the temperature range 25 ℃-60 ℃. Moreover, the adsorption of TRE is chemisorption. The adsorption behavior of TRE follows the Langmuir adsorption isotherm theory. Polarization studies showed TRE was a mixed type inhibitor and the values of effective capacitance were obtained by EIS in the range of double layer capacitance.

ACKNOWLEDGEMENTS
This work was financially supported by the National Natural Sciences Foundation of China (No 2090618), the Natural Sciences Foundation of Hebei province. (No B2010000027) and Talent Program of CNOOC energy development co LTD.

References

1. F. Bentiss, M. Lagrenee, M. Traisnel and J. Hornez, *Corrosion*, 55 (1999) 968.
2. M. Quraishi and D. Jamal, *Corrosion*, 56 (2000) 983.
3. Y. Jiang, Y. Chen, Z. Ye, H. Chen, Z. Zhang, J. Zhang and C. Cao, *Corrosion*, 69 (2013) 672.
4. J. Yu, F. Gan and L. Jiang, *Corrosion*, 64 (2008) 900.
5. M. Tourabi, K. Nohair, M. Traisnel, C. Jama and F. Bentiss, *Corros. Sci.*, 75 (2013) 123.
6. P. B. Raja, M. Fadaeinasab, A. K. Qureshi, A. Rahim, H. Osman, M. Litaudon and K. Awang, *Ind. Eng. Chem. Res.*, 52 (2013) 10582.
7. A. Ostovari, S. Hoseinieh, M. Peikari, S. Shadizadeh and S. Hashemi, *Corros. Sci.*, 51 (2009) 1935.
8. M. Lebrini, F. Robert, A. Lecante and C. Roos, *Corros. Sci.*, 53 (2011) 687.
9. M. Lebrini, F. Robert, P. Blandinières and C. Roos, *Int. J Electrochem. Sc.*, 6 (2011) 2443.
10. M. Lebrini, F. Robert and C. Roos, *Int. J Electrochem. Sc.*, 6 (2011) 847.
11. P. Mourya, S. Banerjee and M. Singh, *Corros. Sci.*, 85 (2014) 352.
12. A. Satapathy, G. Gunasekaran, S. Sahoo, K. Amit and P. Rodrigues, *Corros. Sci.*, 51 (2009) 2848.
13. P. B. Raja and M. G. Sethuraman, *Mater. Lett.*, 62 (2008) 113.
14. O.K. Abiola and A. James, *Corros. Sci.*, 52 (2010) 661.
15. A. Abdel-Gaber, B. Abd-El-Nabey and M. Saadawy, *Corros. Sci.*, 51 (2009) 1038.
16. J. C. D. Rocha, J. A. D. Cunha Ponciano Gomes and E. D'Elia, *Corros. Sci.*, 52 (2010) 2341.
17. A. El-Etre, *Corros. Sci.*, 45 (2003) 2485.

18. A. Abdel-Gaber, B. Abd-El-Nabey, I. Sidahmed, A. El-Zayady and M. Saadawy, *Corros. Sci.*, 48 (2006) 2765.
19. P. B. Raja, A. A. Rahim, H. Osman and K. Awang, *Acta Phys&Chim Sin*, 26 (2010) 2171.
20. M. Lebrini, F. Robert and C. Roos, *Int. J Electrochem. Sc.*, 5 (2010) 1698.
21. M. Faustin, M. Lebrini, F. Robert and C. Roos, *Int. J Electrochem. Sc.*, 6 (2011) 4095.
22. M. Faustin, A. Maciuk, P. Salvin, C. Roos and M. Lebrini, *Corros. Sci.*, 92 (2015) 287.
23. E. E. Oguzie, *Corros. Sci.*, 50 (2008) 2993.
24. P. B. Raja and M. G. Sethuraman, *Mater. Lett.*, 62 (2008) 2977.
25. G. D. Davis, J. Fraunhofer, L. A. Krebs and C. M. Dacres, *Corrosion*, 58(2001) 1558.
26. C. Loto, R. Loto and A. Popoola, *Int. J Electrochem. Sc.*, 6 (2011) 3830.
27. J. Zhao, N. Zhang, C. Qu, X. Wu, J. Zhang and X. Zhang, *Ind. Eng. Chem. Res.*, 49 (2010) 3986.
28. A. Fouda, G. Elewady, K. Shalabi and S. Habouba, *IJAR*, 2 (2014) 817.
29. Z. Švob Troje, Z. Fröbe and Đ. Perović, *J. Chromatogr. A.*, 775 (1997) 101.
30. Y. Guo, H. Wang and Z. Liu, *CIESC J.*, 65 (2014) 298.
31. T. J. Clark and J. E. Bunch, *JCS*, 35 (1997) 209.
32. M. Keinänen, N. J. Oldham and I. T. Baldwin, *J. Agr. Food. Chem.*, 49 (2001) 3553.
33. K. Torikaiu, Y. Uwano, T. Nakamori, W. Tarora and H. Takahashi, *Food. Chem. Toxicol.*, 43 (2005) 559.
34. X. H. Li, S. D. Deng and H. Fu, *J. Appl. Electrochem.*, 40 (2010) 1641.
35. E. Pretsch, P. Bühlmann, C. Affolter, E. Pretsch, P. Bhuhlmann and C. Affolter, *Springer*, 2009.
36. L. Chauhan and G. Gunasekaran, *Corros. Sci.*, 49 (2007) 1143.
37. G. Gunasekaran and L. Chauhan, *Electrochim. Acta*, 49 (2004) 4387.
38. S. Umoren, I. Obot, E. Ebenso and P. Okafor, *Port. Electrochim. Acta*, 26 (2008) 267.
39. X. H. Li, X. G. Xie, S. D. Deng and G. B. Du, *Corros. Sci.*, 92 (2015) 136.
40. S. K. Shukla and M. Quraishi, *Corros. Sci.*, 52 (2010) 314.
41. Y. Harek and L. Larabi, *Kem. Ind.*, 53 (2004) 55.
42. E. A. Noor, *Int. J. Electrochem. Sc.*, 2 (2007) 996.
43. A. Popova, E. Sokolova, S. Raicheva and M. Christov, *Corros. Sci.*, 45 (2003) 33.
44. M. Bimbi, P. Alvarez, H. Vaca and C. Gervasi, *Corros. Sci.*, 92 (2015) 192.
45. E. E. Oguzie, C. B. Adindu, C. K. Enenebeaku, C. E. Ogukwe, M. A. Chidiebere and K. L. Oguzie, *J. Phys. Chem. C.*, 116 (2012) 13603.
46. X. H. Li and G. N. Mu, *Appl. Surf. Sci.*, 252 (2005) 1254.
47. E. Ating, S. Umoren, I. Udousoro, E. Ebenso and A. Udoh, *Green Chem. Lett. Rev.*, 3 (2010) 61.
48. P. M. Krishnegowda, V. T. Venkatesha, P. K. M. Krishnegowda and S. B. Shivayogiraju, *Ind. Eng. Chem. Res.*, 52 (2013) 722.
49. I. Uwah, P. Okafor and V. Ebiekpe, *Arab. J. Chem.*, 6 (2013) 285.
50. M. Gopiraman, N. Selvakumaran, D. Kesavan, I. S. Kim and R. Karvembu, *Ind. Eng. Chem. Res.*, 51 (2012) 7910.
51. H. Jafari, I. Danaee, H. Eskandari and M. RashvandAvei, *Ind. Eng. Chem. Res.*, 52 (2013) 6617.
52. A. Biswas, S. Pal and G. Udayabhanu, *Appl. Surf. Sci.*, 353 (2015) 173.
53. J. Bockris, D. Zic and A. Despic, *Electrochim. Acta*, 4 (1961) 325
54. G. Sığırcık, T. Tüken and M. Erbil, *Appl. Surf. Sci.*, 324 (2015) 232.
55. N. Odewunmi, S. Umoren and Z. Gasem, *JECE*, 3 (2015) 286.
56. L. Ries, M. D. Belo, M. Ferreira and I. Muller, *Corros. Sci.*, 50 (2008) 968.
57. K. Khaled and M. Al-Qahtani, *Mater. Chem. Phys.*, 113 (2009) 150.
58. Z. Tao, W. He, S. Wang and G. Zhou, *Corros. Sci.*, 60 (2012) 205.
59. F. Souza and A. Spinelli, *Corros. Sci.*, 51 (2009) 642.
60. E. A. Flores, O. Olivares, N. V. Likhanova, M. A. Domínguez-Aguilar, N. Nava, D. Guzman-Lucero and M. Corrales, *Corros. Sci.*, 53 (2011) 3899.

61. M. Behpour, S. Ghoreishi, N. Soltani, M. Salavati-Niasari, M. Hamadanian and A. Gandomi, *Corros. Sci.*, 50 (2008) 2172.
62. M. Lebrini, M. Lagrenée, M. Traisnel, L. Gengembre, H. Vezin and F. Bentiss, *Appl. Surf. Sci.*, 253 (2007) 9267.
63. A. Galtayries, R. Warocquier-Clérout, D. Nagel and P. Marcus, *Surf. Interface Anal.*, 38 (2006) 186.
64. K. Boumhara, M. Tabyaoui, C. Jama and F. Bentisset, *J. Ind. Eng. Chem.*, 29 (2015) 146.
65. W. Temesghen and P. Sherwood, *Anal. Bioanal. Chem.*, 373 (2002) 601.
66. M. Chevalier, F. Robert, N. Amusant, M. Traisnel, C. Roos and M. Lebrini, *Electrochim. Acta*, 131 (2014) 96.